Environmental and Experimental Botany 243 (2026) 106326

Contents lists available at ScienceDirect

Environmental and Experimental Botany

journal homepage: www.elsevier.com/locate/envexpbot

Research paper

Light quality affects diurnal gas exchange but not diurnal deacidification in CAM leaves

Stijn Daems [a,b], Rune Keysers [a], Bram Van de Poel [b,c], Johan Ceusters [a,b,d,*]

[a] Research Group for Sustainable Crop Production & Protection, Division of Crop Biotechnics, Department of Biosystems, KU Leuven, Kleinhoefstraat 4, Geel 2440, Belgium
[b] KU Leuven Plant Institute (LPI), KU Leuven, Kasteelpark Arenberg 31, Leuven 3001, Belgium
[c] Division of Crop Biotechnics, Department of Biosystems, KU Leuven, Willem de Croylaan 42, Leuven 3001, Belgium
[d] Centre for Environmental Sciences, Environmental Biology, UHasselt, Diepenbeek 3590, Belgium

ARTICLE INFO

Keywords:
Crassulacean acid metabolism (CAM)
Gas exchange
Kalanchoë fedtschenkoi
Light quality
Malate decarboxylation
Malate remobilisation
Stomatal conductance

ABSTRACT

During the light period, crassulacean acid metabolism (CAM) plants remobilise malic acid from the vacuole and decarboxylate it to supply CO_2 for Rubisco behind closed stomata. Whilst it has been well documented that diurnal deacidification depends strongly on light availability, the impact of light quality on daytime leaf gas exchange and deacidification remains poorly understood. The obligate CAM model species *Kalanchoë fedtschenkoi* was subjected to either different monochromatic wavelengths (blue, green, red) or modified full-spectrum (white) light spectra with a particular waveband omitted (blue, orange, red, far-red, blue+red). Leaf gas exchange parameters and different biochemical parameters associated with diurnal deacidification [i.e., malate and starch content, *in vitro* activities of malic enzyme (ME), pyruvate orthophosphate dikinase (PPDK), and Rubisco] were measured at dawn, midday, and late afternoon. Under high light intensities of 300 μmol m^{-2} s^{-1}, blue wavelengths were found to be a key determinant in promoting high daytime stomatal conductance (Phases II and IV), resulting in improved C_3 carboxylation. Furthermore, omitting red wavelengths from the light spectrum led to a substantially higher overall diel CO_2 uptake (+300 %) compared to plants subjected to spectra lacking either blue or both blue and red wavelengths. In contrast to the large impact on leaf gas exchange, light spectral composition had only a minor impact on diurnal changes in intrinsic enzyme activities of NAD(P)-ME, PPDK, and Rubisco. Consistent with these observations, the diurnal malate degradation and starch accumulation rates were remarkably similar under different spectral compositions. Our findings reveal that stomatal behavior and gas exchange are primarily influenced by light quality, with a more pronounced role for blue compared to red wavelengths. The core biochemical events associated with diurnal deacidification are mainly influenced by light intensity and rather insensitive to changes in spectral composition.

1. Introduction

Crassulacean acid metabolism (CAM) is a specialized mode of photosynthesis, which is present in nearly 7 % of all vascular plants (Gilman et al., 2023). Unlike C_3 and C_4 photosynthetic species, CAM plants open their stomata mainly at night and close them during the major part of the light period, enabling them to minimize transpirational water losses and thrive in arid and semi-arid environments (Borland et al., 2009, 2011, 2014). At night, atmospheric CO_2 is converted to bicarbonate (HCO_3^-) by carbonic anhydrase (CA) which is subsequently fixed onto phospho*enol*pyruvate (PEP) by phospho*enol*pyruvate carboxylase (PEPC) (CAM Phase I; Osmond, 1978). The required PEP is provided via glycolytic breakdown of storage carbohydrates (starch or soluble sugars) accumulated during the previous day. The final 4-C product, malic acid, is stored in the vacuole overnight, leading to substantial vacuolar acidification (Lüttge and Smith, 1984; Franco et al., 1990). During daytime, malate is remobilised and decarboxylated either via mitochondrial and/or cytosolic/chloroplastic NAD(P)-malic enzyme (ME) or a combination of malate dehydrogenase (MDH) and PEPcarboxykinase (PEPCK), depending on the species (CAM Phase III). ME-type

* Corresponding author at: Research Group for Sustainable Crop Production & Protection, Division of Crop Biotechnics, Department of Biosystems, KU Leuven, Kleinhoefstraat 4, Geel 2440, Belgium.
E-mail addresses: stijn.daems@kuleuven.be (S. Daems), runekeysers@gmail.com (R. Keysers), bram.vandepoel@kuleuven.be (B. Van de Poel), johan.ceusters@kuleuven.be (J. Ceusters).

https://doi.org/10.1016/j.envexpbot.2026.106326
Received 9 December 2025; Received in revised form 1 February 2026; Accepted 6 February 2026
Available online 7 February 2026

CAM plants require pyruvate orthophosphate dikinase (PPDK) to convert ME-derived pyruvate to PEP, thereby initiating gluconeogenic recovery of storage carbohydrates (Dever et al., 2015). Following malate decarboxylation, CO_2 is released within the mesophyll tissue and refixed by ribulose 1,5-bisphosphate carboxylase/oxygenase (Rubisco) behind closed stomata. These major CAM Phases (I and III) are usually flanked by Phase II at the start of the day and Phase IV at the end of the day where stomata gradually close and reopen, respectively (Borland and Taybi, 2004). These transitional phases allow CAM plants to show a considerable physiological plasticity to anticipate different environmental perturbations (Lin and Hsu, 2004; Ceusters et al., 2011, 2021b; Tay et al., 2019).

Whilst the nocturnal processes of initial CO_2 fixation, malate biosynthesis and vacuolar storage have been well documented, much less information exists on the diurnal process of malate remobilisation and its regulation (Ceusters et al., 2021a; Winter and Smith, 2022). In this respect, light availability is considered to be one of the key environmental factors (Kluge, 1968; Barrow and Cockburn, 1982; Thomas et al., 1987; Daems et al., 2025). Dever et al. (2015) showed that *Kalanchoë fedtschenkoi* uses mitochondrial NAD-ME as its major decarboxylase for CAM in the light period. In addition, together with their later work reported in Boxall et al. (2020), the Hartwell group demonstrated the differential regulation over the light/dark cycle of PPDK by dephosphorylation/phosphorylation by PPDK-regulatory protein (-RP) in a CAM species. PPDK was dephosphorylated (activated) at the start of the light period and was phosphorylated (inactivated) at the end of the light period, coinciding with the completion of malate decarboxylation. More recently, the recycling enzyme PPDK has been proposed as a potential key regulator of light-dependent diurnal deacidification in CAM leaves, given its marked sensitivity to light intensity and photoperiod at the mRNA, protein, and enzyme activity levels in *K. fedtschenkoi*, closely matching diurnal malate dynamics (Daems et al., 2025). Apart from light intensity and photoperiod, also the spectral composition of light (light quality) might impact CAM biochemistry and physiology (e.g., Ceusters et al., 2014; Zheng et al., 2019; Zhang et al., 2020).

There is no doubt that the CAM pathway is affected by light quality, which implies crucial roles for particular photoreceptors (i.e., phytochromes, phototropins, cryptochromes, zeitlupes or UV RESISTANCE LOCUS 8 (UVR8)) in synchronising metabolism over the diel cycle. The red light photoreceptor phytochrome has been demonstrated to play a pivotal role in maintaining the CAM-defining circadian rhythms of CO_2 fixation under red light, as first shown in *Bryophyllum fedtschenkoi* by Harris and Wilkins (1976), (1978a), (1978b). Furthermore, phytochromes seemed also involved in the short-photoperiod induction of CAM in *Kalanchoë blossfeldiana* (Queiroz, 1969; Brulfert et al., 1973, 1982, 1988; Taybi et al., 2002). However, *Phalaenopsis* plants exposed to only red light for 8 weeks exhibited remarkably lower nocturnal CO_2 fixation, reduced malate accumulation, consistently lower diurnal malate decarboxylation rates, and prolonged malate degradation extending up to 4 h after dusk. Intrinsic PEPC activity remained unaffected by monochromatic red light, which suggested that the adverse effects under red light were likely caused by restricted availability of storage carbohydrates such as starch (Zheng et al., 2019).

The function of blue light photoreceptors in the operation and synchronization of the metabolic pathway of CAM is still largely uncertain. No detectable effect of blue light on the persistence, phase, or period of the rhythm of CO_2 metabolism in *Bryophyllum* leaves was noted by Wilkins (1992), suggesting a minor role for the blue/UV-A absorbing cryptochromes and phototropins in the synchronization of CAM phases. In contrast, it has been suggested that a UV-A/blue light receptor governs the high PPFD-induced switch from C_3 to CAM in *Clusia minor* (Grams and Thiel, 2002). In addition, the apparent blue-light insensitivity of CAM stomata reported for the facultative CAM species *Portulacaria afra* and *Mesembryanthemum crystallinum* has been proposed as a central component for ensuring daytime stomatal closure during CAM Phase III (Lee and Assmann, 1992; Mawson and Zaugg, 1994; Tallman et al., 1997). These observations might suggest a possible C_3 to CAM divergence in light signaling pathways mediated by blue light photoreceptors (Ceusters et al., 2014). However, more recent findings seem to challenge the blue light-insensitive stomata hypothesis and indicate effective roles for blue light in mediating gas exchange and photosynthesis-related phenomena in CAM plants. The phototropin-mediated blue light signaling cascade and related activation of the guard cell plasma membrane H^+-ATPase and subsequent stomatal opening, as known from C_3 and C_4 species, seems conserved in the obligate CAM species *K. pinnata* and *K. daigremontiana* (Gotoh et al., 2019). Lin et al. (2019) also demonstrated that phototropins mediate blue light-dependent chloroplast movements in the orchid *Phalaenopsis aphrodite*. However, their function appears to differ somewhat from that in Arabidopsis, since heterologous expression of *PaPHOT1* or *PaPHOT2* in an Arabidopsis *phot1phot2* double mutant failed to restore the chloroplast avoidance response during high light intensities. In addition, Ceusters et al. (2014) reported that both blue and red light input signals are required for optimal coupling of stomatal conductance, net CO_2 uptake, and the reciprocal turnover of carbohydrates and organic acids over the diel CAM cycle.

Taken together, it is clear that many questions remain concerning the influence of light quality on CAM. To shed more light onto the immediate effects of light quality on CAM physiology and biochemistry, this study aimed to uncover whether, and how, light quality affects diurnal leaf gas exchange and modulates diurnal deacidification in CAM leaves of *K. fedtschenkoi* over the short term (single-day treatment). To achieve this, we employed an integrative analysis that spanned physiological (gas exchange), temporal metabolic, and enzyme activity levels. We hypothesize that diurnal CAM physiology and biochemistry are differently affected by different spectral light qualities in the short term.

2. Materials and methods

2.1. Plant material and growth conditions

Kalanchoë fedtschenkoi Hamet et Perrier plants were propagated clonally from leaf margin adventitious plantlets and were grown in groups of four in 3.4 L pots containing universal potting soil (De Ceuster Meststoffen NV, Belgium). Plants were cultivated for ca. 12 weeks in controlled growth rooms with a 12 h photoperiod (from 08:00 until 20:00 h), day/night temperature of 23/18 °C, 75 % relative humidity (RH), and photosynthetically active radiation (PAR) at the apex of ~300 μmol m^{-2} s^{-1} which was provided by LED growth lamps with broad wavelength spectra (Mars Hydro TSL-2000: https://marshydro.eu/) until reaching the 12-leaf pairs (LP) stage. This standard white light spectrum is shown in Fig. 1b. Watering was performed twice a week using tap water and plants were maintained under ambient CO_2 concentrations.

2.2. Light quality treatments and temporal sampling

Two separate light quality experiments were performed to investigate the effects of light quality on diurnal malate remobilisation and its associated processes (i.e., stomatal conductance and gas exchange, leaf malate and starch dynamics, and intrinsic activities of NAD(P)-ME, PPDK, and Rubisco). The first experiment was based on different monochromatic light treatments, whilst the second included the use of different light spectra in which a particular waveband was omitted from a full-spectrum (white) light background (different spectral compositions). Custom-made multispectral LED lamps capable of illuminating 16 different wavelengths in various ratios were used (wavelength range: 370–740 nm; Carendes BV, Haasrode, Belgium) to develop the diverse light spectra (Fig. 1, Table 1). Consistent with the growth conditions, the lamps were switched on at 08:00 h and switched off at 20:00 h.

Whilst plants were cultivated under ~300 μmol m^{-2} s^{-1}, the maximal light intensity achievable with monochromatic lights was

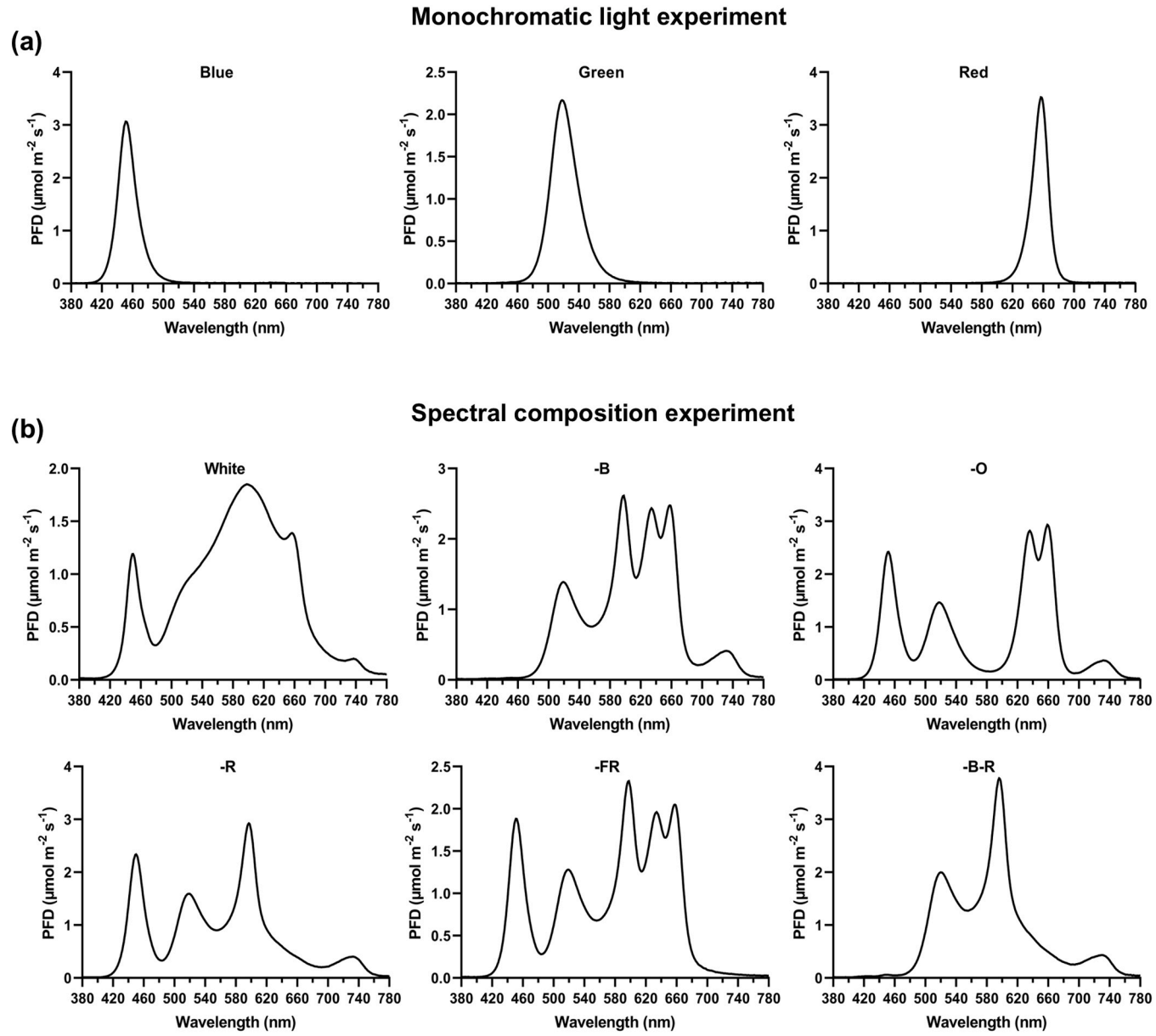

Fig. 1. Spectra of the applied light treatments. Spectral photon distribution of the applied light treatments normalised to a photon flux density (PFD) of 100 µmol m^{-2} s^{-1} for monochromatic Blue, Green, and Red (monochromatic light experiment) (a), and to a PFD of 300 µmol m^{-2} s^{-1} for White, -B, -O, -R, -FR, -B-R (spectral composition experiment) (b).

Table 1
Spectral photon distribution (in %) of the applied light treatments in the spectral composition experiment normalized to a photon flux density (PFD) of 300 µmol m^{-2} s^{-1}. Blue 400–500 nm, green 500–600 nm, red 600–700 nm, and far-red (FR) 700–800 nm as a fraction of the PFD in the range 400–800 nm. Abbreviations are: -B, white light spectrum lacking the blue waveband; -O, white light spectrum lacking the orange waveband; -R, white light spectrum lacking the red waveband; -FR, white light spectrum lacking the far-red waveband; -B-R, white light spectrum lacking the blue and red wavebands.

Light treatment	Blue	Green	Red	Far-red	B:G ratio	R:FR ratio
White (Mars Hydro)	14 %	42 %	40 %	4 %	0,33	10,0
-B	3 %	40 %	51 %	6 %	0,08	8,5
-O	25 %	22 %	48 %	5 %	1,14	9,6
-R	25 %	47 %	22 %	6 %	0,53	3,7
-FR	20 %	36 %	43 %	1 %	0,55	43,0
-B-R	4 %	62 %	28 %	6 %	0,06	4,7

limited to 100 µmol m^{-2} s^{-1}. Therefore, a 100 µmol m^{-2} s^{-1} white light control was also included in the monochromatic light experiment. Treatments in this experiment included: full-spectrum white, blue (B, 450 nm), green (G, 520 nm), and red (R, 660 nm) at 100 µmol m^{-2} s^{-1} (Fig. 1a).

For the experiment subjecting the plants to different spectral compositions, an equal total light intensity at the apex across all treatments of 300 µmol m^{-2} s^{-1} was ensured by compensating for a particular omission of a waveband by increasing the intensity of the remaining wavebands. Treatments in the experiment with different spectral compositions included: full-spectrum white (White = control), white spectrum lacking blue wavelengths (-B), white spectrum lacking orange wavelengths (-O), white spectrum lacking red wavelengths (-R), white spectrum lacking far-red wavelengths (-FR), and a white spectrum lacking both blue and red wavelengths (-B-R). Light intensities were checked using a handheld full-spectrum quantum meter (Apogee MQ-501). The spectral compositions of the applied light treatments were

measured with a PAR200 Quantum Spectrometer (UPRTEK) and are provided in Fig. 1b and Table 1. Light treatments were separated with black cloth that allowed air and moisture to pass through in the growth chamber, but prevented any light penetration between the different compartments.

Separate but uniform batches of plants were used for both experiments. Plants were treated for only one photoperiod and samples were randomly taken from leaf pairs 5, 6, and 7 (LP5, 6, 7; with LP1 starting from the apex) at dawn (7:45 h, 15 min before the lights were switched on), midday (13:00 h) and late afternoon (17:00 h). Five biological replicates were taken at each time point and were snap frozen in liquid nitrogen, powdered and stored at −80 °C until further analysis.

2.3. Leaf CO_2 exchange, stomatal conductance, and transpiration measurements

Gas exchange parameters (net CO_2 uptake, stomatal conductance, and transpiration) were measured randomly on leaf pairs 5, 6, and 7 (counted down from the apex). Leaves were placed into a broad leaf chamber (6.25 cm^2, light-transmitting) of the LCi Portable Photosynthesis System (ADC BioScientific Ltd., United Kingdom) 1 h before the start of the photoperiod. Incoming light intensity was measured using the integrated PAR sensor in the LCi Portable Photosynthesis System and this data is presented in Supporting Information Table S1. The flow rate of air was set at 68 μmol m^{-2} s^{-1} and the incoming air was passed through a 20-L bottle to buffer short-term fluctuations in ambient CO_2 levels. Leaf temperatures were consistent among the different treatments within an experiment (monochromatic and different spectral compositions) and are presented in Supporting Information Table S2. The calculated vapour pressure deficit was 0.88 kPa (monochromatic experiment) and 1.25 kPa (spectral compositions experiment) during daytime, and 0.79 kPa during the night in both experiments. Gas exchange data were collected over the diel cycle with measurements obtained at 15-min intervals. Each gas exchange curve presented is representative of data obtained from 3 to 5 independent biological replicates. By integrating specific areas under the gas exchange curves [CO_2 and transpiration (H_2O)], net gas exchange was calculated for day and night as well as total net gas exchange during the 24 h period.

2.4. Biochemical analyses of metabolites

Metabolite analyses were performed on leaf samples taken at 7:45, 13:00, and 17:00 h (n = 5). Starch was extracted by heating frozen, powdered leaf tissue in 80 % methanol to 80 °C for 40 min. The insoluble pellet was used for starch determination, following digestion by amyloglucosidase and α-amylase as described by Haider et al. (2012) and assayed spectrophotometrically at 340 nm as glucose equivalents (Daems et al., 2022). Extraction and measurement of malic acid was performed as described by Chen et al. (2002), with modifications as described in Daems et al. (2022).

2.5. Enzyme activity assays for NAD-ME, NADP-ME, PPDK, and Rubisco

Enzyme activity analyses were performed on leaf samples collected at 7:45 and 17:00 h (n = 5). PPDK activity was also measured in leaf samples taken at 13:00 h given its pronounced temporal regulation in *K. fedtschenkoi* (Daems et al., 2025). Extraction and assay for mitochondrial NAD-ME, cytosolic/plastidic NADP-ME, and PPDK were based on the methods described by Dever et al. (2015), with slight modifications as described below. The extraction and assay of Rubisco were based on the method described by Borland et al. (1998), with slight modifications as described below. All extraction steps were performed by homogenizing powdered leaf material at 4 °C in the enzyme-specific extraction buffer. Samples were centrifuged at 16,200 *g* for 2 min at 4 °C in a microfuge. The supernatant was utilized either directly, or first desalted by passing twice through a column of Sephadex G-25 for the NAD-ME assay.

The NAD-ME extraction buffer comprised 100 mM HEPES-KOH, pH 7.0, 2 mM $MnCl_2$, 5 mM DTT, 1 % polyvinylpyrrolidone-40, 1 mM EDTA, 2 % PEG-20000, and 0.5 % Triton X-100. The desalting buffer contained 125 mg/mL Sephadex G-25 (Sigma-Aldrich), 100 mM HEPES-KOH, pH 7.0, 2 mM $MnCl_2$, 5 mM DTT, and 1 mM EDTA. The assay comprised 50 mM HEPES-KOH, pH 7.6, 1 mM EDTA, 1 mM DTT, 5 mM L-malate, 5 mM NAD, 25 μM NADH, 1 U pig heart MDH (Roche Life Sciences), 100 μM acetyl CoA, and 5 mM $MnCl_2$; 25 μM NADH was included to minimize the interference of MDH in the assay and reduce the chance of overestimation of NAD-ME activity (Hatch et al., 1982). After preincubation of extracts for 30 min at 30°C, the reaction was initiated by the addition of extract to the assay and the change in absorbance at 340 nm was measured for 4 min at 25°C. Preliminary experiments confirmed a linear increase of NADH for at least 6 min.

The NADP-ME extraction buffer comprised 200 mM Tricine-NaOH, pH 7.6, 1 mM EDTA, 2 % polyvinylpyrrolidone-40, 2 mM DTT, 1 mM benzamidine hydrochloride, 2 % PEG-20000 plus 50 mg g^{-1} tissue $NaHCO_3$, and 200 mg g^{-1} tissue polyvinylpolypyrrolidone (PVPP). The assay comprised 50 mM HEPES-KOH, pH 7.0, 0.1 mM EDTA, 1 mM $NADP^+$, 10 mM L-malate, 5 mM DTT, and 1 mM $MgCl_2$. After preincubation of extracts for 30 min at 30°C, the reaction was initiated by the addition of extract to the assay and the change in absorbance at 340 nm was measured for 4 min at 25°C. Preliminary experiments confirmed a linear increase of NADPH for at least 6 min.

The PPDK extraction buffer comprised 50 mM HEPES-KOH, pH 8.2, 5 mM DTT, 0.2 mM EDTA, 2 % PEG-20000, 2.5 mM K_2HPO_4, 2.5 mM pyruvate, and 200 mg g^{-1} tissue PVPP. The assay comprised 50 mM Tris-HCl, pH 8.0, 5 mM DTT, 10 mM MgCl2, 1.25 mM pyruvate, 0.25 mM NADH, 2.5 mM $NaHCO_3$, 2.5 mM K_2HPO_4, 1 U pig heart MDH, 1.25 mM ATP, and 6 mM Glc-6-P. The reaction was initiated by the addition of extract to the assay and the change in absorbance at 340 nm was measured for 4 min at 25°C. Preliminary experiments confirmed a linear decrease of NADH for at least 6 min.

The Rubisco extraction buffer contained 400 mM HEPES-KOH, pH 7.5, 5 mM EGTA, 5 mM $MgCl_2$, 2 % (w/v) PEG-20000, 14 mM β-mercaptoethanol, 16 mg PVPP, and 1 mM PMSF. The initial activity of Rubisco was assayed in a reaction mix that comprised 100 mM Bicine-KOH, pH 8.0, 25 mM $NaHCO_3$, 20 mM $MgCl_2$, 3.5 mM ATP, 3.5 mM P-creatine, 0.25 mM NADH, 5 U 3-phosphoglyceric phosphokinase, 5 U glyceraldehyde 3-phosphate dehydrogenase, and 5 U creatine phosphokinase. After preincubation for 10 min at 25°C, the reaction was initiated by the addition of RuBP to a final concentration of 0.5 mM and the change in absorbance at 340 nm was measured for 4 min at 25°C. Preliminary experiments confirmed a linear decrease of NADH for at least 6 min.

2.6. Statistical analyses

Data analysis was performed using SPSS 28.0 (IBM, New York, NY, USA). Before carrying out statistical tests, normality and equality of variances of the data were checked by means of a Shapiro-Wilk and Levene's test ($p > 0.05$), respectively. Means of two groups were compared by a two sample *t*-test. Means of three or more groups were compared by ANOVA followed by Tukey's HSD post-hoc test ($p < 0.05$). The non-parametric Kruskal-Wallis test, followed by Dunn's post-hoc test, was used if the conditions were not met.

3. Results

3.1. Leaf diel stomatal conductance, CO_2 exchange, and transpiration are strongly affected by light quality

3.1.1. Stomatal conductance

Plants exposed to monochromatic blue and green light at 100 μmol m^{-2} s^{-1} exhibited markedly higher peak stomatal conductances at dawn

(Phase II) compared to plants under 100 μmol m^{-2} s^{-1} white and monochromatic red light (Fig. 2a). However, stomatal conductances of all plants remained low in the afternoon and lacked the CAM-associated increase typically observed during Phase IV. Nocturnal stomatal conductances were comparable among all light treatments (Fig. 2a).

For plants exposed to the different 300 μmol m^{-2} s^{-1} spectra, stomatal conductance patterns appeared to cluster into two distinct groups during the diurnal period (Fig. 2b). The first group, consisting of light treatments containing blue wavelengths (i.e., White, -O, -R, -FR), displayed higher stomatal conductances as well as a typical CAM pattern, with pronounced peaks during Phases II and IV. The second group, including light treatments lacking blue wavelengths (i.e., -B and -B-R), showed markedly reduced stomatal conductances. Nighttime stomatal conductances were broadly comparable across all light treatments (Fig. 2b).

3.1.2. CO_2 exchange

Reducing the light intensity from 300 μmol m^{-2} s^{-1} (growth light intensity) to 100 μmol m^{-2} s^{-1} resulted in negative diurnal photosynthesis rates and almost eliminated net CO_2 uptake over the diel cycle (Fig. 2c; Table 2a). At this lower intensity, plants subjected to either white light or the three monochromatic light treatments (B, G, R) showed fairly similar diel CO_2 exchange curves (Fig. 2c, Table 2a).

When exposed to different spectral compositions at the higher PPFD of 300 μmol m^{-2} s^{-1}, all plants exhibited typical CAM CO_2 exchange patterns, characterized by nocturnal CO_2 fixation (Phase I), net CO_2 loss during the middle of the photoperiod (Phase III), and two transitional phases at dawn and dusk respectively showing net uptake (Phases II and

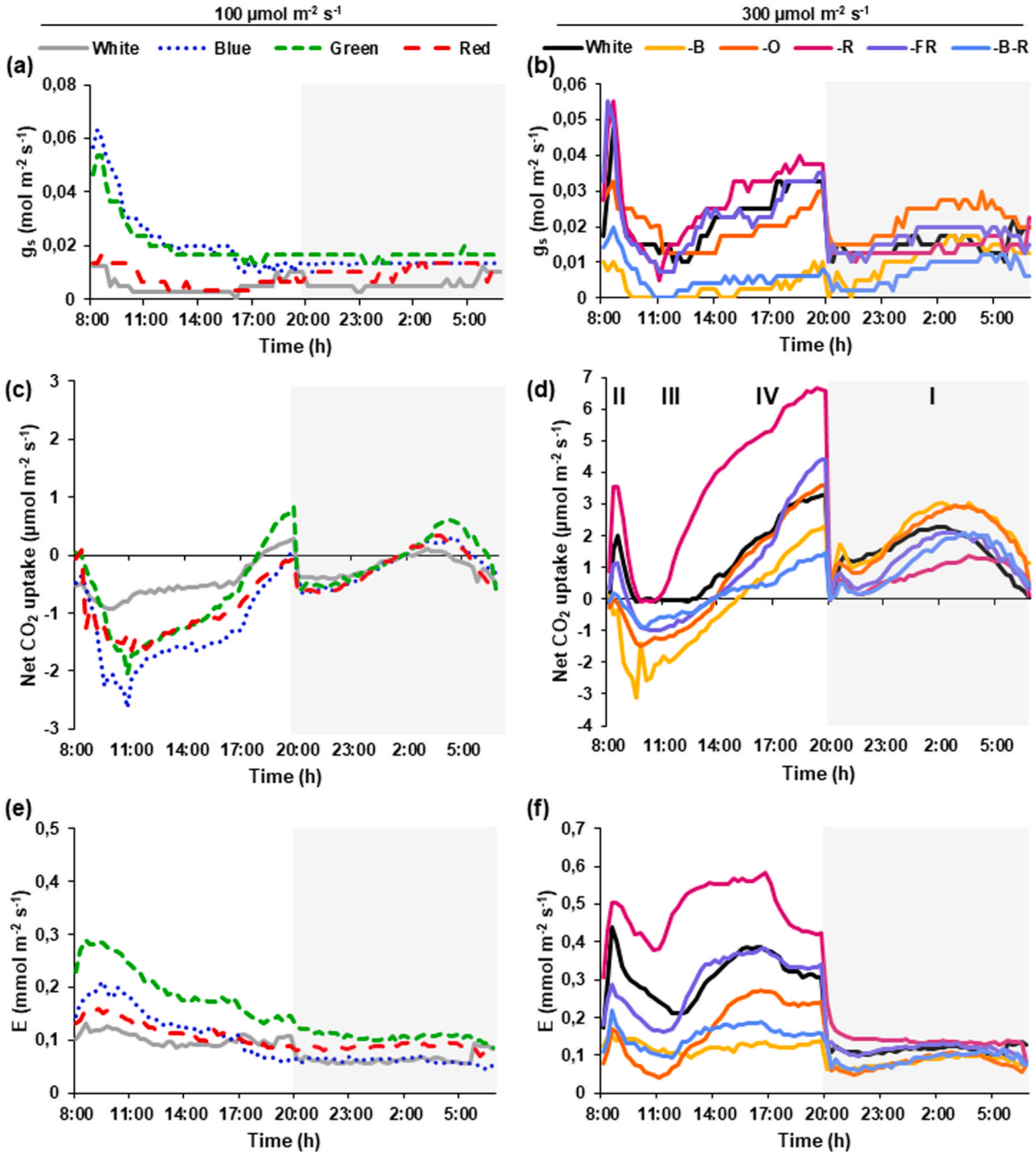

Fig. 2. Diel gas exchange data for *Kalanchoë fedtschenkoi* leaves exposed to either a reduced white light control and reduced monochromatic lights (a, c, e), or light spectra with equal light intensities but with a particular waveband omitted (b, d, f) for one day. Diel stomatal conductance (mol m^{-2} s^{-1}) (a, b), net 24 h CO_2 uptake (μmol m^{-2} s^{-1}) (c, d), and net 24 h transpiration (mmol m^{-2} s^{-1}) (e, f) measured randomly for leaf pairs 5, 6, or 7 (n = 3–5 plants). The dark period is indicated in grey. Roman numbers above Fig. 2d indicate the different CAM phases.

Table 2
Diurnal, nocturnal, and diel leaf gas exchange data (net CO_2 uptake and transpiration) for *Kalanchoë fedtschenkoi* exposed to either a reduced white light control and reduced monochromatic lights (a), or light spectra with equal light intensities but with a particular waveband omitted (b) for one day. Gas exchange was measured randomly for leaf pairs 5, 6, or 7. Data are means ± SD (n = 3–5 plants). Values were compared among the light treatments per column (day/night/total) according to Tukey's HSD test at $p < 0.05$ marked by different letters.

(a)

	Photosynthesis (mmol m^{-2})			Transpiration (mol m^{-2})		
Light treatment (100 µmol m^{-2} s^{-1})	**DAY**	**NIGHT**	**TOTAL**	**DAY**	**NIGHT**	**TOTAL**
White	-20 ± 12^{a}	-8 ± 7^{a}	-28 ± 19^{a}	4,4 ± 1,3^{a}	2,6 ± 0,7^{ab}	7,0 ± 2,0^{a}
Blue	-57 ± 7^{a}	-7 ± 9^{a}	-64 ± 11^{a}	5,6 ± 0,8^{a}	2,4 ± 0,5^{b}	8,0 ± 1,0^{a}
Green	-33 ± 30^{a}	-3 ± 9^{a}	-36 ± 39^{a}	8,6 ± 6,5^{a}	5,3 ± 2,0^{a}	13,9 ± 8,4^{a}
Red	-43 ± 10^{a}	-8 ± 21^{a}	-51 ± 24^{a}	5,0 ± 1,5^{a}	3,5 ± 0,9^{ab}	8,5 ± 2,3^{a}

(b)

	Photosynthesis (mmol m^{-2})			Transpiration (mol m^{-2})		
Light treatment (300 µmol m^{-2} s^{-1})	**DAY**	**NIGHT**	**TOTAL**	**DAY**	**NIGHT**	**TOTAL**
White	54 ± 17^{b}	59 ± 18^{ab}	112 ± 16^{ab}	13,3 ± 2,2^{ab}	4,6 ± 0,6^{ab}	17,9 ± 2,3^{ab}
-B	-13 ± 15^{b}	83 ± 19^{a}	71 ± 13^{b}	5,3 ± 0,9^{b}	3,3 ± 0,6^{b}	8,6 ± 1,4^{b}
-O	28 ± 32^{b}	77 ± 33^{ab}	105 ± 52^{ab}	7,3 ± 7,2^{b}	3,2 ± 0,9^{b}	10,6 ± 7,8^{b}
-R	155 ± 57^{a}	32 ± 17^{b}	187 ± 45^{a}	21,0 ± 5,7^{a}	5,6 ± 1,3^{a}	26,6 ± 6,6^{a}
-FR	40 ± 57^{b}	50 ± 17^{ab}	90 ± 61^{ab}	12,6 ± 2,9^{ab}	4,6 ± 0,9^{ab}	17,3 ± 2,7^{ab}
-B-R	7 ± 31^{b}	44 ± 10^{ab}	51 ± 34^{b}	6,6 ± 5,1^{b}	3,5 ± 0,8^{ab}	10,1 ± 5,8^{b}

IV) (Fig. 2d). However, both the amplitude and duration of the different CAM phases were strongly influenced by the spectral composition (Fig. 2d). Plants exposed to the light spectrum lacking red wavelengths (-R) showed a significantly higher daytime CO_2 fixation compared to all other light spectra, but their nocturnal CO_2 fixation was lower (ca. −60 %) than that of plants under the spectrum lacking blue wavelengths (-B) (Fig. 2d, Table 2b). Omitting red wavelengths from the light spectrum (-R) led to a higher overall diel CO_2 uptake (+300 %) compared to plants subjected to spectra lacking either blue (-B) or both blue and red (-B-R) wavelengths (Fig. 2d, Table 2b). Plants under light spectra lacking either orange (-O) or far-red (-FR) wavelengths exhibited diel CO_2 uptake patterns comparable to controls (Fig. 2d, Table 2b).

3.1.3. Transpiration

Plants exposed to 100 µmol m^{-2} s^{-1} white or monochromatic light (B, G, R) showed similar kinetics and rates of transpiration (Fig. 2e, Table 2a). Monochromatic green light seemed to stimulate daytime transpiration (Fig. 2e), although this was not significantly different from white light (Table 2a).

Transpirational water loss in the spectral composition experiment matched the CAM-specific patterns of CO_2 uptake and stomatal conductance (Fig. 2f). Plants subjected to the spectrum lacking red wavelengths (-R) showed remarkably higher transpiration rates during daytime and the diel cycle compared to those under light spectra lacking either blue (-B), orange (-O), or both blue and red (-B-R) wavelengths (Fig. 2f, Table 2b). Nighttime transpiration rates were slightly higher under the light spectrum lacking red wavelengths (-R) compared to spectra without blue (-B) or orange (-O) wavelengths (Fig. 2f, Table 2b).

3.2. The influence of light quality on malate degradation and starch accumulation is limited

As expected, leaf malate levels were high at dawn (7:45 h, ca. 50 µmol g^{-1}FW) in all treatment groups (Fig. 3). Reduced light intensities of 100 µmol m^{-2} s^{-1} brought about a small, but significant degree of malate degradation (ca. 10 µmol g^{-1}FW between 7:45 and 17:00 h), except under the monochromatic green light (Fig. 3a). All 300 µmol m^{-2} s^{-1} spectra also initiated a significant, but remarkably higher and equal malate consumption for the different treatments during the day (ca. 36 µmol g^{-1}FW) (Fig. 3b). Moderate malate levels of ca. 27 µmol g^{-1}FW were observed at 13:00 h which further declined to ca. 14 µmol g^{-1}FW at 17:00 h.

Leaf starch content exhibited a typical pattern opposite to that of malate, with low levels at dawn (ca. 3 µmol g^{-1}FW) across all treatments (Fig. 4). In plants subjected to 100 µmol m^{-2} s^{-1} white or monochromatic red light, starch levels significantly increased by ca. 10 µmol g^{-1}FW towards 13:00 h and remained stable afterwards (Fig. 4a). Under monochromatic blue light, starch accumulation was delayed until 17:00 h, whilst no significant increase occurred under monochromatic green light (Fig. 4a).

Under 300 µmol m^{-2} s^{-1}, starch accumulation rates were not affected by the light spectral composition. Plants accumulated about 25 µmol g^{-1}FW towards 13:00 h, which further increased significantly to about 50 µmol g^{-1}FW at 17:00 h (Fig. 4b).

3.3. Enzymes involved in diurnal malate decarboxylation, CO_2 fixation and carbohydrate recycling show a remarkable flexibility with respect to light quality

Mitochondrial NAD-ME displayed intrinsic baseline activities of about 13 µmol PYR h^{-1} g^{-1}FW at 7:45 h, which significantly increased towards ca. 20 µmol PYR h^{-1} g^{-1}FW at 17:00 h under all 100 µmol m^{-2} s^{-1} treatments (Fig. 5a). A significant diurnal increase in NAD-ME activity was also observed in all plants exposed to the different light spectra at high light intensities of 300 µmol m^{-2} s^{-1} (Fig. 5b). At 17:00 h, NAD-ME activity levels were comparable across all spectra (ca. 24 µmol PYR h^{-1} g^{-1}FW), except in plants exposed to the spectrum lacking both blue and red light (-B-R), which exhibited significantly lower activity (ca. 21 µmol PYR h^{-1} g^{-1}FW) compared to those under the spectrum lacking far-red (-FR) (Fig. 5b).

Cytosolic/chloroplastic NADP-ME showed low baseline activities of ca. 2 µmol PYR h^{-1} g^{-1}FW at 7:45 h and its activity slightly increased towards ca. 3 µmol PYR h^{-1} g^{-1}FW at 17:00 h for all treatments in both experiments, except under monochromatic green light (Fig. 5c, d). NADP-ME activities at 17:00 h were similar between the control white spectrum and different spectra with an omitted waveband (Fig. 5d).

Under reduced 100 µmol m^{-2} s^{-1} monochromatic light, Rubisco activities increased significantly from ca. 5 µmol CO_2 h^{-1} g^{-1}FW at 7:45 h to ca. 8 µmol CO_2 h^{-1} g^{-1}FW at 17:00 h, except under monochromatic green light (Fig. 5e). Under high light intensities, Rubisco activity of control plants showed a stronger increase from ca. 5 µmol CO_2 h^{-1} g^{-1}FW at 7:45 h towards ca. 10 µmol CO_2 h^{-1} g^{-1}FW at 17:00 h (Fig. 5f). This trend was also observed in plants subjected to spectra lacking far-red (-FR) or both blue and red (-B-R) wavelengths but was absent under spectra lacking blue (-B), orange (-O) or red (-R) wavelengths (Fig. 5f).

PPDK activity was very low at dawn (7:45 h) (ca. 1 µmol PEP h^{-1} g^{-1}FW) in all plants in both experiments (Fig. 5g, h). Reduced light intensities caused PPDK activity to gradually increase throughout the light phase (ca. 2 and 3.5 µmol PEP h^{-1} g^{-1}FW at 13:00 h and 17:00 h respectively), for all treatments except for the monochromatic green light (Fig. 5g). A stronger increasing and comparable trend for all treatments was also observed under the different high intensity spectra

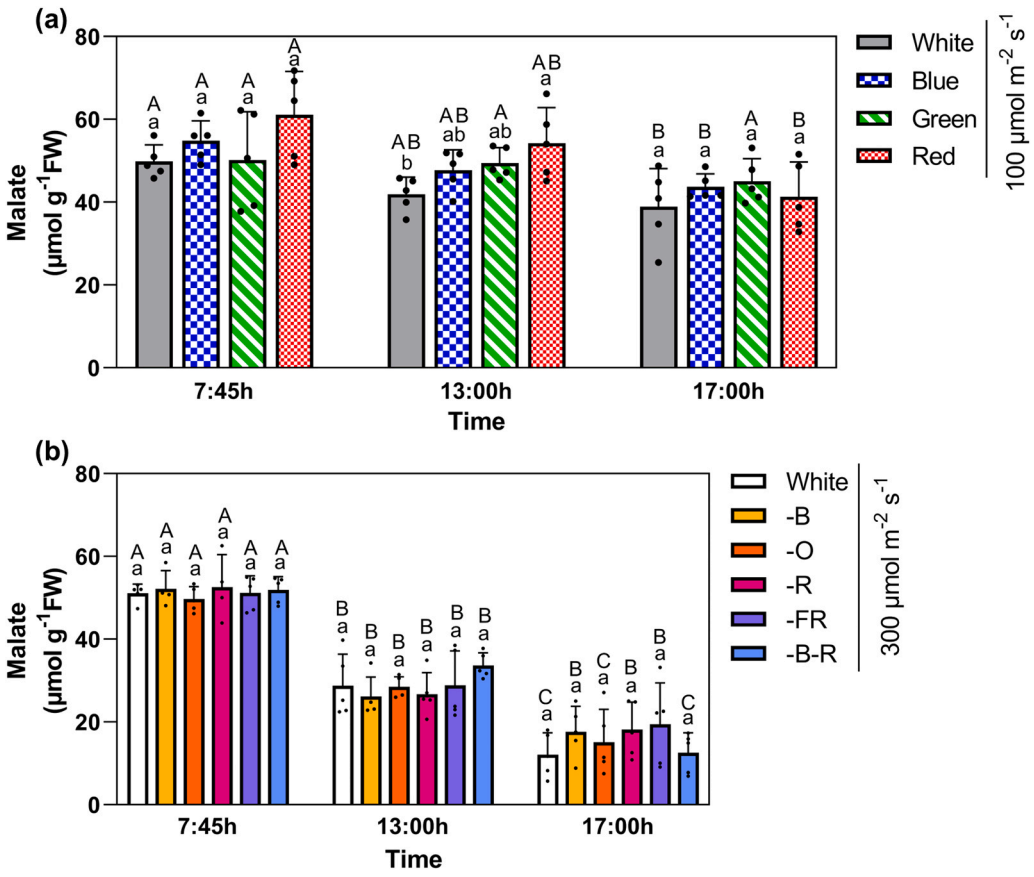

Fig. 3. Temporal patterns of leaf malate concentrations. Malate (µmol g^{-1}FW) measured for leaf pairs 5, 6, or 7 of *Kalanchoë fedtschenkoi* exposed to either a reduced white light control and reduced monochromatic lights (a) or light spectra with equal light intensities but with a particular waveband omitted (b) for one day. Samples were collected at time points 7:45 h (dawn), 13:00 h (midday) and 17:00 h (late afternoon). Data are means ± SE (n = 5 plants). Values were compared among the different treatments per time point according to Tukey's HSD test at $p < 0.05$ marked by different lower case letters and among the different time points per treatment marked by different capital letters.

where activities reached ca. 7 µmol PEP h^{-1} g^{-1}FW at 13:00 h and ca. 9 µmol PEP h^{-1} g^{-1}FW at 17:00 h (Fig. 5h).

4. Discussion

Whilst the impact of light availability on diurnal deacidification in CAM leaves has been acknowledged for a long time (Kluge, 1968; Barrow and Cockburn, 1982; Thomas et al., 1987; Daems et al., 2025), the immediate effects of light quality have received less attention. This study therefore aimed to uncover the short-term impact of light quality on leaf gas exchange and different biochemical processes related to diurnal deacidification in *K. fedtschenkoi*. To detect and untangle possible interactions between different light colors, we combined monochromatic experiments with different additional polychromatic treatments, each lacking a particular waveband.

4.1. Stomatal conductance and gas exchange are mainly influenced by the proportion of blue light in the light spectrum

Under high light intensities of 300 µmol m^{-2} s^{-1}, stomatal conductances during the daytime Phases II and IV were consistently lower under light spectra containing only a small fraction of blue light (<4 %, -B and -B-R) compared to all other treatments with > 14 % blue wavelengths (White, -O, -R, -FR) (Fig. 2b) (see spectra in Fig. 1 and Table 1). These findings highlight an essential role for blue light in promoting stomatal opening during daytime and thereby stimulating C_3 carboxylation during Phases II and IV. A pronounced peak stomatal conductance at dawn under monochromatic blue light at 100 µmol m^{-2} s^{-1} further corroborates this view (Fig. 2a). Stomatal conductance and C_3 carboxylation were unaffected by the presence or absence of red wavelengths in light spectra lacking blue wavelengths (-B and -B-R) (Fig. 2b, d, Table 2b). In contrast, these parameters displayed remarkable changes depending on the presence of blue wavelengths in light spectra lacking red wavelengths (-R and -B-R). These observations suggest that blue light is the primary factor promoting stomatal conductance and C_3 carboxylation, whilst red light acts as a secondary factor with a potential suppressive effect on C_3 carboxylation. Furthermore, whilst Phase IV stomatal conductances were all similar for the White, -O, -R, and -FR treatments, transpiration rates were clearly different (Fig. 2f). Since leaf temperatures were also similar under all treatments (Table S2), light quality might also impact other potential transpiration-related processes such as aquaporin transcript abundance in leaves (Ben Baaziz et al., 2012) and/or rates of photo-assimilate translocation (Lanoue et al., 2018).

It has previously been shown that the stomata of some facultative CAM species were unresponsive to blue light, based on studies using individual leaves or epidermal peels from *Portulacaria afra* and *Mesembryanthemum crystallinum*, where blue light-induced stomatal opening was absent after CAM induction (Lee and Assmann, 1992; Mawson and Zaugg, 1994; Tallman et al., 1997). In contrast, our present study aligns with more recent works reporting blue light-triggered stomatal opening in the obligate CAM plants *Aechmea* 'Maya', *K. pinnata* and *K. daigremontiana* (Ceusters et al., 2014; Gotoh et al., 2019). At the molecular level, blue light has been found to increase transcript levels of the photoreceptors *PHOT1* and *PHOT2* at both dawn and dusk in *K. fedtschenkoi* (Zhang et al., 2020). In addition, most stomatal

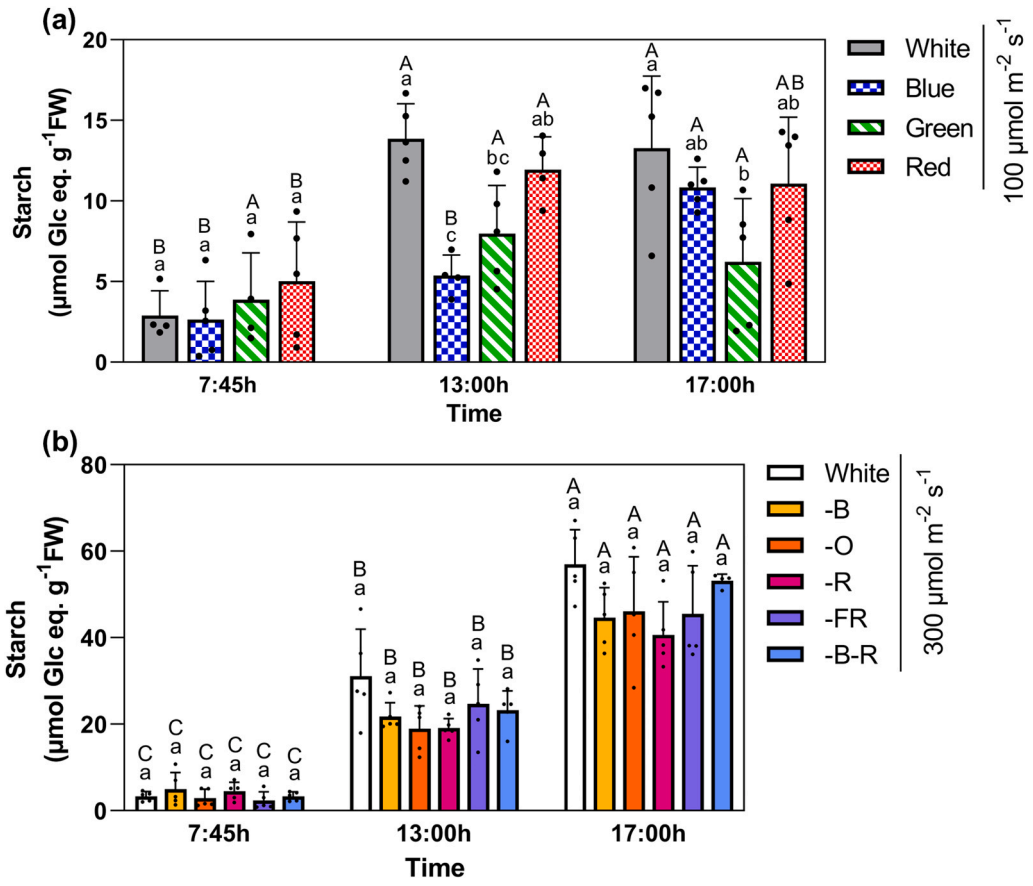

Fig. 4. Temporal patterns of starch content in leaves. Starch contents (µmol Glc eq. g^{-1}FW) measured for leaf pairs 5, 6, or 7 of *Kalanchoë fedtschenkoi* exposed to either a reduced white light control and reduced monochromatic lights (a) or light spectra with equal light intensities but with a particular waveband omitted (b) for one day. Leaf samples were collected at time points 7:45 h (dawn), 13:00 h (midday) and 17:00 h (late afternoon). Data are means ± SE (n = 5 plants). Values were compared among the different treatments per time point according to Tukey's HSD test at $p < 0.05$ marked by different lower case letters and among the different time points per treatment marked by different capital letters.

movement-associated genes (e.g., *ABI2*, *ALMT9*, *KAT1*, *KAT2*, and *QUAC1/ALMT12*) were found to be induced by blue light, particularly at dawn (Zhang et al., 2020). Collectively, the findings presented here, along with previous research, provide strong evidence that blue light-dependent stomatal opening does occur in at least certain obligate CAM species, similar to C_3 and C_4 plants (Shimazaki et al., 2007).

However, a notable difference in blue light-dependent guard cell metabolism between C_3 and CAM plants has been reported. In Arabidopsis, blue light triggers early-photoperiod starch degradation in guard cells, producing malate that serves as a counter ion for K^+ influx during stomatal opening (Streb and Zeeman, 2012; Santelia and Lunn, 2017). This mechanism is absent in *K. fedtschenkoi*, where no such starch breakdown was detected and early-photoperiod stomatal opening was independent of starch degradation in both guard and mesophyll cells (Abraham et al., 2020; Hurtado-Castano et al., 2023). Remarkably, none of the 100 µmol m^{-2} s^{-1} treatments showed a peak in Phase IV stomatal conductance (Fig. 2a), suggesting that, in addition to light quality, a threshold light intensity is also essential to accommodate Phase IV stomatal opening. This also indicates a certain role for guard cell and/or mesophyll cell photosynthetic metabolism in mediating stomatal behavior. It has been shown that guard cells of *K. fedtschenkoi* are capable of sensing light intensity directly (Santos et al., 2021). Adding to the complexity of stomatal regulation, stomatal responses to light intensity in CAM plants were found to be modulated by an unknown signal originating from the mesophyll, as also observed in C_3 and C_4 plants (Santos et al., 2021). Future work at the cell type-specific level is required to uncover the impact of light intensity and light quality on the interplay between CAM mesophyll and guard cell malate and starch metabolism, and putative associated impact on stomatal behavior.

Besides the transitional Phases II and IV, also daytime Phase III was clearly affected by a reduction in light intensity from 300 µmol m^{-2} s^{-1} (growth light intensity) to 100 µmol m^{-2} s^{-1}. Strong negative photosynthesis rates were consistently registered during Phase III, irrespective of the light quality (Fig. 2c; Table 2a). Since diurnal malate decarboxylation was still observed under this lower light intensity (about 10.6 µmol malate g^{-1} FW degraded between 8:00 and 17:00 h; Fig. 3a) and Rubisco activation is expected to be reduced under low light (Zhang and Portis, 1999), the negative carbon balance at 100 µmol m^{-2} s^{-1} likely reflects higher diffusional CO_2 losses from the mesophyll cells. Also, the fact that malate decarboxylation rates generally exceeded starch accumulation rates (about 6.7 µmol starch g^{-1} FW accumulated between 8:00 and 17:00 h; Fig. 4a) point towards the possibility that at least some of the ME-derived pyruvate enters the TCA cycle for respiration, liberating extra CO_2. Elucidating how reduced light intensity exactly affects the interplay of these different biochemical events related to malate decarboxylation and the putative associated CO_2 release from CAM mesophyll cells remains a key topic for future research.

From all treatments with high diurnal stomatal conductances (i.e., light spectra with high proportions of blue light), the spectrum with the lowest amount of red light (-R; 22 % red) brought about an earlier commencement of Phase IV and an increase in the maximum rate of direct atmospheric CO_2 assimilation (Fig. 2b, d, Table 2b). The higher C_3 carboxylation under -R is unlikely attributable to a lower R:FR ratio, nor to the possible involvement of phytochromes. The -B-R treatment, which lacked both blue and red wavelengths and had a similar low R:FR ratio, did not exhibit increased diurnal CO_2 uptake (Fig. 2d, Tables 1, 2b).

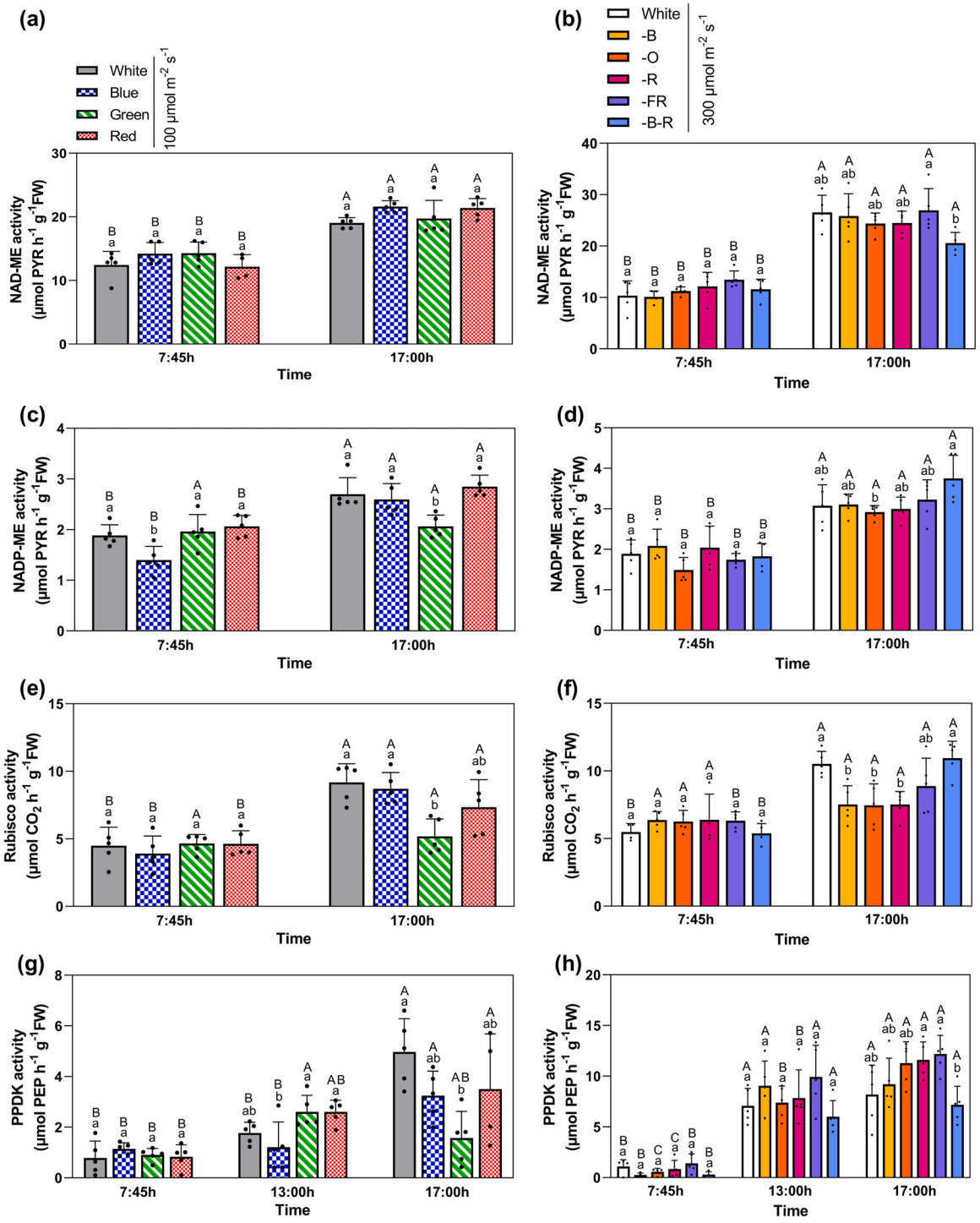

Fig. 5. Temporal intrinsic activity data of enzymes involved in diurnal malate decarboxylation, CO_2 fixation and carbohydrate recycling. Diurnal enzyme activity data for mitochondrial NAD-ME (µmol PYR h^{-1} g^{-1}FW) (a), cytosolic/chloroplastic NADP-ME (µmol PYR h^{-1} g^{-1}FW) (c), Rubisco (µmol CO_2 h^{-1} g^{-1}FW) (e), and PPDK (µmol PEP h^{-1} g^{-1}FW) (g) at 7:45 h (dawn) and 17:00 h (late afternoon) measured for leaf pairs 5, 6, or 7 of *Kalanchoë fedtschenkoi* exposed to a reduced white light control and different reduced monochromatic lights for one day. Diurnal enzyme activity data for NAD-ME (b), NADP-ME (d), Rubisco (f), and PPDK (h) at 7:45 h (dawn) and 17:00 h (late afternoon) measured for leaf pairs 5, 6, or 7 of *K. fedtschenkoi* exposed to different light spectra with equal light intensities but with a particular waveband omitted for one day. PPDK activity was also measured at 13:00 h given its pronounced temporal regulation in *K. fedtschenkoi* (see Materials and methods, Daems et al., 2025). Data are means ± SE (n = 5 plants). Values were compared among the different treatments per time point according to Tukey's HSD test at $p < 0.05$ marked by different lower case letters and among the different time points per treatment marked by different capital letters.

Furthermore, despite the fact that -O and -FR spectra had markedly different R:FR ratios (Table 1), plants under these spectra displayed comparable stomatal conductances and gas exchange (Fig. 2b, d, f). The higher daytime CO_2 uptake under -R did also not appear to result from increased Rubisco activity, as intrinsic activity under this spectrum was comparable to, or even slightly lower than, those for the other treatments (Fig. 5f). On the photosynthetic level, red light has been shown to reduce both maximum quantum yield (F_v/F_m) and quantum efficiency (Φ_{PSII}) in the short term in the CAM orchid *Phalaenopsis* (Zheng et al., 2019). This indicates that under red light the light reactions of

photosynthesis might not be optimal, potentially restricting ATP and NADPH availability for the Calvin-Benson-Bassham (CBB) cycle. Also in C_3 species, monochromatic red light is generally found to reduce photosynthetic electron transport capacity and CO_2 assimilation, along with reduced mRNA levels and activities of CBB cycle-associated enzymes, compared to white, monochromatic blue, or combined R and B illumination (Hogewoning et al., 2010; Miao et al., 2016, 2019; Trouwborst et al., 2016; Li et al., 2020). In contrast, blue light has been shown to increase transcript levels of several CBB cycle genes in the C_3 species *Cucumis sativus* (Wang et al., 2009), likely mediated by cryptochromes, which promote the expression of multiple CBB cycle genes (Mishra and Khurana, 2017; Kochetova et al., 2022).

4.2. Biochemistry of diurnal deacidification is remarkably consistent among different light spectra

In contrast to the clear differences in stomatal conductance and gas exchange patterns under different light spectra, spectral composition did not seem to exert marked effects on biochemical events associated with the diurnal deacidification processes. The significantly higher C_3 carboxylation observed under the -R spectrum did not result in higher starch levels at dusk compared to all other light treatments (Fig. 4b). This suggests that (1) malate accumulated during the preceding night was likely converted to pyruvate and starch in a consistent 1:1 stoichiometric ratio across all treatments and (2) the extra carbon assimilated during the day under the -R spectrum was probably directed toward sucrose biosynthesis, subsequently loaded into the phloem and transported to sink tissues. This seems plausible since light quality is known to impact several aspects of sucrose metabolism and source-sink transport in C_3 species. For example, in tomato, sucrose synthase activity was highest under a spectrum containing red and blue light in a 3:1 ratio (Li et al., 2017). Far-red light has been found to increase fruit sink strength due to upregulation of sugar transport and metabolism genes in tomato (Ji et al., 2020). The molecular basis of these light quality-dependent responses remains to be elucidated in CAM species.

The remarkably consistent rates in malate degradation and starch accumulation among the different light spectra were also reflected in the diurnal changes of intrinsic activities of different acid degradation-related enzymes (Figs. 3b, 4b, 5b, d, f, h). Activities of enzymes involved in decarboxylation (i.e. NAD(P)-ME and PPDK) and refixation (Rubisco) were strikingly similar under the different spectral compositions. Even with lower proportions of both blue and red wavelengths (-B-R) (see spectra in Fig. 1 and Table 1), which are most efficiently absorbed by photosynthetically active pigments, plants were still able to degrade malate and accumulate starch to levels comparable to white light controls (Figs. 3b, 4b). Diurnal increases in intrinsic enzyme activities comparable to controls were also noticed under this -B-R spectrum (Fig. 5b, d, f, h). In addition, our results demonstrate that green and orange wavelengths were also effective in accommodating diurnal deacidification, underscoring a large flexibility of *K. fedtschenkoi* in terms of light spectral composition towards diurnal deacidification given a sufficiently high PPFD.

In early studies about the effects of light quality on CAM, Nalborczyk et al. (1975) suggested a putative role for phytochrome in diurnal deacidification, as far-red light was found to stimulate malate decarboxylation in *K. daigremontiana*. However, even under a substantially lower proportion of FR light (R:FR ratio of 10 under control white light vs 43 under -FR, Table 1), malate degradation, starch accumulation rates, and diurnal changes in intrinsic activities of enzymes potentially involved in malate remobilisation were not abolished. In the facultative CAM species *M. crystallinum*, exposure to light with a low R:FR ratio (in contrast to light with a high R:FR ratio), caused induction of PEPC activity, accumulation of the CAM isoform of PEPC, and nocturnal malate accumulation, suggesting a role for phytochrome in the signal transduction pathway underlying CAM induction (Cockburn et al., 1996). However, in our study with *K. fedtschenkoi*, treatments with either a low R:FR ratio (-R and -B-R) or a high R:FR ratio (-FR, ratio=43) exhibited similar levels of nocturnal CO_2 fixation—as a proxy for CAM expression—compared to controls (Table 2b). These observations might suggest a possible photoreceptor signaling divergence between facultative and obligate CAM species.

White light and different monochromatic wavelengths at the lower PPFD of 100 μmol m^{-2} s^{-1} showed similar levels of significantly induced malate degradation, starch accumulation, and diurnal alterations in intrinsic enzyme activity (Figs. 3a, 4a, 5a, c, e, g). Monochromatic green light was an exception, as it did not induce malate degradation or starch accumulation and plants exhibited lower intrinsic NADP-ME, Rubisco and PPDK activities at dusk. This aligns with observations in C_3 species, where monochromatic green light has been found to stimulate net photosynthetic rate to a lesser extent, reduce Rubisco content, reduce starch and soluble sugar levels compared to monochromatic blue and red, and to impair PSII activity (Wu et al., 2014; Yang et al., 2016; Liu et al., 2023). In addition, the absolute dawn-dusk differences in metabolite concentrations and enzyme activities observed under the 100 μmol m^{-2} s^{-1} treatments were remarkably smaller than those observed under 300 μmol m^{-2} s^{-1} treatments, indicating that light intensity exerts a greater impact on diurnal malate remobilisation than light quality. Consistent with this view, PPDK has earlier been identified as a potential key regulator of light-dependent diurnal deacidification in CAM leaves given its marked sensitivity to light intensity and photoperiod at the mRNA, protein, and enzyme activity levels in *K. fedtschenkoi*, closely matching diurnal malate dynamics (Daems et al., 2025). In our present study, PPDK activities seem indeed rather insensitive to light spectral composition (Fig. 5h). These findings strengthen the idea that PPDK regulation is primarily influenced by light intensity and photoperiod rather than photoreceptor-mediated signaling. Uncovering the molecular mechanisms underlying these light intensity and photoperiod-associated responses are key areas for future investigation. Whilst low-fluence blue light (10 μmol m^{-2} s^{-1}) has been reported to induce malate degradation but not starch accumulation in the obligate CAM bromeliad *A.* 'Maya' (Ceusters et al., 2014), we demonstrate that blue light at a higher intensity of 100 μmol m^{-2} s^{-1} stimulated both diurnal deacidification-related processes (Figs. 3a, 4a). Similarly, although low-fluence red light was shown to trigger starch accumulation but not malate degradation in *A.* 'Maya', we showed that red light at a higher intensity of 100 μmol m^{-2} s^{-1} also induced both processes (Figs. 3a, 4a). These observations further emphasize the importance of light intensity and its underlying connection to the light reactions of photosynthesis, accommodating energy and redox homeostasis and orchestrating diurnal carbohydrate turnover in CAM plants.

In summary, light spectral composition affected daytime leaf gas exchange in the short term mainly through its influence on stomatal behavior. In contrast, the core biochemical events of diurnal deacidification (i.e., malate degradation, starch accumulation and intrinsic activities of different key enzymes potentially involved) were primarily influenced by light intensity, rather than light spectral composition. These observations urge for a deeper understanding of how light quality and light intensity shape the molecular regulation of stomatal behavior, diurnal deacidification and carbon metabolism and partitioning in CAM species.

Author contributions

JC, SD and BVdP designed the research. RK and SD performed the experiments and collected the data. All authors analysed data. SD and JC wrote the paper. SD created the figures. All authors revised the manuscript and approved the final version.

CRediT authorship contribution statement

Johan Ceusters: Writing – review & editing, Writing – original draft, Supervision, Project administration, Funding acquisition, Formal

analysis, Conceptualization. **Stijn Daems:** Writing – review & editing, Writing – original draft, Visualization, Investigation, Formal analysis, Data curation, Conceptualization. **Rune Keysers:** Investigation, Formal analysis, Data curation. **Bram Van de Poel:** Writing – review & editing, Supervision, Formal analysis.

Declaration of Competing Interest

The authors declare that they have no known competing financial interests or personal relationships that could have appeared to influence the work reported in this paper.

Acknowledgements

The authors are especially thankful to Kim Vekemans for her support with the gas exchange measurements. Funding was provided by the Research Fund KU Leuven to JC (C14/21/067) and BVdP (C14/18/056).

Appendix A. Supporting information

Supplementary data associated with this article can be found in the online version at doi:10.1016/j.envexpbot.2026.106326.

Data availability

The authors declare that all data supporting the findings of this study are available within the paper and its Supporting Information files (Tables S1-S2).

References

Abraham, P.E., Hurtado Castano, N., Cowan-Turner, D., et al., 2020. Peeling back the layers of crassulacean acid metabolism: functional differentiation between Kalanchoë fedtschenkoi epidermis and mesophyll proteomes. Plant J. Cell Mol. Biol. 103, 869–888.

Barrow, S.R., Cockburn, W., 1982. Effects of light quantity and quality on the decarboxylation of malic acid in crassulacean acid metabolism photosynthesis. Plant Physiol. 69, 568–571.

Ben Baaziz, K., Lopez, D., Rabot, A., et al., 2012. Light-mediated Kleaf induction and contribution of both the PIP1s and PIP2s aquaporins in five tree species: walnut (Juglans regia) case study. Tree Physiol. 32, 423–434.

Borland, A.M., Taybi, T., 2004. Synchronization of metabolic processes in plants with Crassulacean acid metabolism. J. Exp. Bot. 55, 1255–1265.

Borland, A.M., Técsi, L.I., Leegood, R.C., Walker, R.P., 1998. Inducibility of crassulacean acid metabolism (CAM) in Clusia species; physiological/biochemical characterisation and intercellular localization of carboxylation and decarboxylation processes in three species which exhibit different degrees of CAM. Planta 205, 342–351.

Borland, A.M., Griffiths, H., Hartwell, J., Smith, J.A.C., 2009. Exploiting the potential of plants with crassulacean acid metabolism for bioenergy production on marginal lands. J. Exp. Bot. 60, 2879–2896.

Borland, A.M., Barrera Zambrano, V.A., Ceusters, J., Shorrock, K., 2011. The photosynthetic plasticity of crassulacean acid metabolism: an evolutionary innovation for sustainable productivity in a changing world. N. Phytol. 191, 619–633.

Borland, A.M., Hartwell, J., Weston, D.J., et al., 2014. Engineering crassulacean acid metabolism to improve water-use efficiency. Trends Plant Sci. 19, 327–338.

Boxall, S.F., Kadu, N., Dever, L.V., Kneřová, J., Waller, J.L., Gould, P.J.D., Hartwell, J., 2020. Kalanchoë PPC1 is essential for crassulacean acid metabolism and the regulation of core circadian clock and guard cell signaling genes[CC-BY]. Plant Cell 32, 1136–1160.

Brulfert, J., Guerrier, D., Queiroz, O., 1973. Photoperiodism and enzyme activity: balance between inhibition and induction of the crassulacean acid metabolism. Plant Physiol. 51, 220–222.

Brulfert, J., Müller, D., Kluge, M., Queiroz, O., 1982. Photoperiodism and crassulacean acid metabolism. Planta 154, 326–331.

Brulfert, J.I. de P.V., Kluge, M., Gueclue, S., Queiroz, O., 1988. Interaction of photoperiod and drought as CAM inducing factors in Kalanchoe blossfeldiana Poelln., cv. Tom Thumb. J. Plant Physiol. 133, 222–227.

Ceusters, J., Borland, A.M., Godts, C., et al., 2011. Crassulacean acid metabolism under severe light limitation: a matter of plasticity in the shadows? J. Exp. Bot. 62, 283–291.

Ceusters, J., Borland, A.M., Taybi, T., Frans, M., Godts, C., De Proft, M.P., 2014. Light quality modulates metabolic synchronization over the diel phases of crassulacean acid metabolism. J. Exp. Bot. 65, 3705–3714.

Ceusters, N., Borland, A.M., Ceusters, J., 2021a. How to resolve the enigma of diurnal malate remobilisation from the vacuole in plants with crassulacean acid metabolism? N. Phytol. 229, 3116–3124.

Ceusters, N., Ceusters, J., Hurtado-Castano, N., et al., 2021b. Phosphorolytic degradation of leaf starch via plastidic α-glucan phosphorylase leads to optimized plant growth and water use efficiency over the diel phases of Crassulacean acid metabolism. J. Exp. Bot. 72, 4419–4434.

Chen, L., Lin, Q., Nose, A., 2002. A comparative study on diurnal changes in metabolite levels in the leaves of three crassulacean acid metabolism (CAM) species, Ananas comosus, Kalanchoë daigremontiana and K. pinnata. J. Exp. Bot. 53, 341–350.

Cockburn, W., Whitelam, G.C., Broad, A., Smith, J., 1996. The participation of phytochrome in the signal transduction pathway of salt stress responses in Mesembryanthemum crystallinum L. J. Exp. Bot. 47, 647–653.

Daems, S., Ceusters, N., Valcke, R., Ceusters, J., 2022. Effects of chilling on the photosynthetic performance of the CAM orchid Phalaenopsis. Front. Plant Sci. 13.

Daems, S., Van de Poel, B., Ceusters, J., 2025. Pyruvate orthophosphate dikinase (PPDK) as a putative key regulator of diurnal deacidification in CAM leaves across varying light intensities and photoperiods. J. Exp. Bot., eraf500

Dever, L.V., Boxall, S.F., Kneřová, J., Hartwell, J., 2015. Transgenic perturbation of the decarboxylation phase of crassulacean acid metabolism alters physiology and metabolism but has only a small effect on growth. Plant Physiol. 167, 44–59.

Franco, A.C., Ball, E., Lüttge, U., 1990. Patterns of gas exchange and organic acid oscillations in tropical trees of the genus Clusia. Oecologia 85, 108–114.

Gilman, I.S., Smith, J.A.C., Holtum, J.A.M., et al., 2023. The CAM lineages of planet Earth. Ann. Bot. 132, 627–654.

Gotoh, E., Oiwamoto, K., Inoue, S., Shimazaki, K., Doi, M., 2019. Stomatal response to blue light in crassulacean acid metabolism plants Kalanchoe pinnata and Kalanchoe daigremontiana. J. Exp. Bot. 70, 1367–1374.

Grams, T.E.E., Thiel, S., 2002. High light-induced switch from C(3)-photosynthesis to Crassulacean acid metabolism is mediated by UV-A/blue light. J. Exp. Bot. 53, 1475–1483.

Haider, M.S., Barnes, J.D., Cushman, J.C., Borland, A.M., 2012. A CAM- and starch-deficient mutant of the facultative CAM species Mesembryanthemum crystallinum reconciles sink demands by repartitioning carbon during acclimation to salinity. J. Exp. Bot. 63, 1985–1996.

Harris, P.J.C., Wilkins, M.B., 1976. Light-induced changes in the period of the circadian rhythm of carbon dioxide output in Bryophyllum leaves. Planta 129, 253–258.

Harris, P.J.C., Wilkins, M.B., 1978a. Evidence of phytochrome involvement in the entrainment of the circadian rhythm of carbon dioxide metabolism in Bryophyllum. Planta 138, 271–278.

Harris, P.J.C., Wilkins, M.B., 1978b. The circadian rhythm in Bryophyllum leaves: Phase control by radiant energy. Planta 143, 323–328.

Hatch, M.D., Tsuzuki, M., Edwards, G.E., 1982. Determination of NAD Malic Enzyme in Leaves of C(4) plants: effects of malate dehydrogenase and other factors. Plant Physiol. 69, 483–491.

Hogewoning, S.W., Trouwborst, G., Maljaars, H., Poorter, H., van Ieperen, W., Harbinson, J., 2010. Blue light dose–responses of leaf photosynthesis, morphology, and chemical composition of Cucumis sativus grown under different combinations of red and blue light. J. Exp. Bot. 61, 3107–3117.

Hurtado-Castano, N., Atkins, E., Barnes, J., et al., 2023. The starch-deficient plastidic PHOSPHOGLUCOMUTASE mutant of the constitutive crassulacean acid metabolism (CAM) species Kalanchoë fedtschenkoi impacts diel regulation and timing of stomatal CO2 responsiveness. Ann. Bot. 132, 881–894.

Ji, Y., Nuñez Ocaña, D., Choe, D., Larsen, D.H., Marcelis, L.F.M., Heuvelink, E., 2020. Far-red radiation stimulates dry mass partitioning to fruits by increasing fruit sink strength in tomato. N. Phytol. 228, 1914–1925.

Kluge, M., 1968. Untersuchungen über den Gaswechsel von Bryophyllum während der Lichtperiode. Planta 80, 359–377.

Kochetova, G.V., Avercheva, O.V., Bassarskaya, E.M., Zhigalova, T.V., 2022. Light quality as a driver of photosynthetic apparatus development. Biophys. Rev. 14, 779–803.

Lanoue, J., Leonardos, E.D., Grodzinski, B., 2018. Effects of light quality and intensity on diurnal patterns and rates of photo-assimilate translocation and transpiration in tomato leaves. Front. Plant Sci. 9.

Lee, D.M., Assmann, S.M., 1992. Stomatal responses to light in the facultative Crassulacean acid metabolism species, Portulacaria afra. Physiol. Plant. 85, 35–42.

Li, Y., Xin, G., Wei, M., Shi, Q., Yang, F., Wang, X., 2017. Carbohydrate accumulation and sucrose metabolism responses in tomato seedling leaves when subjected to different light qualities. Sci. Hortic. 225, 490–497.

Li, Y., Xin, G., Liu, C., Shi, Q., Yang, F., Wei, M., 2020. Effects of red and blue light on leaf anatomy, CO2 assimilation and the photosynthetic electron transport capacity of sweet pepper (Capsicum annuum L.) seedlings. BMC Plant Biol. 20, 318.

Lin, M.-J., Hsu, B.-D., 2004. Photosynthetic plasticity of *Phalaenopsis* in response to different light environments. J. Plant Physiol. 161, 1259–1268.

Lin, Y.-J., Chen, Y.-C., Tseng, K.-C., Chang, W.-C., Ko, S.-S., 2019. Phototropins mediate chloroplast movement in Phalaenopsis aphrodite (Moth Orchid). Plant Cell Physiol. 60, 2243–2254.

Liu, M., Zhao, Y., Fan, P., et al., 2023. Grapevine plantlets respond to different monochromatic lights by tuning photosynthesis and carbon allocation. Hortic. Res. 10, uhad160.

Lüttge, U., Smith, J.A.C., 1984. Mechanism of passive malic-acid efflux from vacuoles of the CAM plantKalanchoë daigremontiana. J. Membr. Biol. 81, 149–158.

Mawson, B.T., Zaugg, M.W., 1994. Modulation of light-dependent stomatal opening in isolated epidermis following induction of crassulacean acid metabolism in *Mesembryanthemum crystallinum* L. J. Plant Physiol. 144, 740–746.

Miao, Y., Wang, X., Gao, L., Chen, Q., Qu, M., 2016. Blue light is more essential than red light for maintaining the activities of photosystem II and I and photosynthetic electron transport capacity in cucumber leaves. J. Integr. Agric. 15, 87–100.
Miao, Y., Chen, Q., Qu, M., Gao, L., Hou, L., 2019. Blue light alleviates 'red light syndrome' by regulating chloroplast ultrastructure, photosynthetic traits and nutrient accumulation in cucumber plants. Sci. Hortic. 257, 108680.
Mishra, S., Khurana, J.P., 2017. Emerging roles and new paradigms in signaling mechanisms of plant cryptochromes. Crit. Rev. Plant Sci. 36, 89–115.
Nalborczyk, E., Lacroix, L.J., Hill, R.D., 1975. Environmental influences on light and dark CO2 fixation by Kalanchoe daigremontiana. Can. J. Bot. 53, 1132–1138.
Osmond, C.B., 1978. Crassulacean acid metabolism: a curiosity in context. Annu. Rev. Plant Physiol. 29, 379–414.
Queiroz, O., 1969. Photoperiodisme et activite enzymatique (PEP carboxylase et enzyme malique) dans les feuilles de Kalanchoe blossfeldiana. Phytochemistry 8, 1655–1663.
Santelia, D., Lunn, J.E., 2017. Transitory starch metabolism in guard cells: unique features for a unique function. Plant Physiol. 174, 539–549.
Santos, M.G., Davey, P.A., Hofmann, T.A., Borland, A., Hartwell, J., Lawson, T., 2021. Stomatal responses to Light, CO2, and Mesophyll Tissue in Vicia faba and Kalanchoë fedtschenkoi. Front. Plant Sci. 12, 740534.
Shimazaki, K., Doi, M., Assmann, S.M., Kinoshita, T., 2007. Light regulation of stomatal movement. Annu. Rev. Plant Biol. 58, 219–247.
Streb, S., Zeeman, S.C., 2012. Starch metabolism in arabidopsis. Arab. Book Am. Soc. Plant Biol. 10, e0160.
Tallman, G., Zhu, J., Mawson, B.T., et al., 1997. Induction of CAM in Mesembryanthemum crystallinum abolishes the stomatal response to blue light and light-dependent zeaxanthin formation in guard cell chloroplasts. Plant Cell Physiol. 38, 236–242.
Tay, S., He, J., Yam, T.W., 2019. CAM plasticity in epiphytic tropical orchid species responding to environmental stress. Bot. Stud. 60, 7.
Taybi, T., Cushman, J.C., Borland, A.M., 2002. Environmental, hormonal and circadian regulation of crassulacean acid metabolism expression. Funct. Plant Biol. 29, 669–678.
Thomas, D.A., Andre, M., Granzin, A.-M., 1987. Oxygen and carbon dioxide exchanges in crassulacean acid metabolism plants. II: Effects of CO2 concentration and irradiance. Oxygen and carbon dioxide exchanges in crassulacean acid metabolism plants. II Eff. CO2 Conc. Irradiance 25, 95–103.
Trouwborst, G., Hogewoning, S.W., van Kooten, O., Harbinson, J., van Ieperen, W., 2016. Plasticity of photosynthesis after the 'red light syndrome' in cucumber. Environ. Exp. Bot. 121, 75–82.
Wang, H., Gu, M., Cui, J., Shi, K., Zhou, Y., Yu, J., 2009. Effects of light quality on CO2 assimilation, chlorophyll-fluorescence quenching, expression of Calvin cycle genes and carbohydrate accumulation in *Cucumis sativus*. J. Photochem. Photobiol. B Biol. 96, 30–37.
Wilkins, M.B., 1992. Tansley review No. 37 Circadian rhythms: their origin and control. N. Phytol. 121, 347–375.
Winter, K., Smith, J.A.C., 2022. CAM photosynthesis: the acid test. N. Phytol. 233, 599–609.
Wu, Q., Su, N., Shen, W., Cui, J., 2014. Analyzing photosynthetic activity and growth of Solanum lycopersicum seedlings exposed to different light qualities. Acta Physiol. Plant. 36, 1411–1420.
Yang, B., Zhou, X., Xu, R., et al., 2016. Comprehensive analysis of photosynthetic characteristics and quality improvement of purple cabbage under different combinations of monochromatic light. Front. Plant Sci. 7, 1788.
Zhang, J., Hu, R., Sreedasyam, A., et al., 2020. Light-responsive expression atlas reveals the effects of light quality and intensity in Kalanchoë fedtschenkoi, a plant with crassulacean acid metabolism. GigaScience 9, giaa018.
Zhang, N., Portis, A.R., 1999. Mechanism of light regulation of Rubisco: a specific role for the larger Rubisco activase isoform involving reductive activation by thioredoxin-f. Proc Natl Acad Sci U S A 96, 9438–9443. https://doi.org/10.1073/pnas.96.16.9438.
Zheng, L., Ceusters, J., Van Labeke, M.-C., 2019. Light quality affects light harvesting and carbon sequestration during the diel cycle of crassulacean acid metabolism in Phalaenopsis. Photosynth. Res. 141, 195–207.